Multimodal neuroimaging relationships in progressive supranuclear palsy

Article *in* Parkinsonism & Related Disorders · July 2019

DOI: 10.1016/j.parkreldis.2019.07.001

11 authors, including:

Irene Sintini
Mayo Clinic - Rochester
12 PUBLICATIONS **44** CITATIONS
SEE PROFILE

Christopher G. Schwarz
Mayo Foundation for Medical Education and Research
169 PUBLICATIONS **1,993** CITATIONS
SEE PROFILE

Matthew L Senjem
Mayo Foundation for Medical Education and Research
405 PUBLICATIONS **13,814** CITATIONS
SEE PROFILE

Robert Ian Reid
Mayo Foundation for Medical Education and Research
70 PUBLICATIONS **781** CITATIONS
SEE PROFILE

Parkinsonism and Related Disorders xxx (xxxx) xxx–xxx

Contents lists available at ScienceDirect

Parkinsonism and Related Disorders

journal homepage: www.elsevier.com/locate/parkreldis

Multimodal neuroimaging relationships in progressive supranuclear palsy

Irene Sintini[a,*], Christopher G. Schwarz[a], Matthew L. Senjem[a,b], Robert I. Reid[b], Hugo Botha[c], Farwa Ali[c], J. Eric Ahlskog[c], Clifford R. Jack Jr.[a], Val J. Lowe[a], Keith A. Josephs[c], Jennifer L. Whitwell[a]

[a] Department of Radiology, Mayo Clinic, Rochester, MN, USA
[b] Department of Information Technology, Mayo Clinic, Rochester, MN, USA
[c] Department of Neurology, Mayo Clinic, Rochester, MN, USA

ARTICLE INFO

Keywords:
PSP
Multimodal imaging
Tau-PET
DTI
MRI

ABSTRACT

Progressive supranuclear palsy is characterized primarily by 4R tau inclusions, atrophy in the brainstem and basal ganglia, and neurodegeneration along the dentatorubrothalamic tract, which are measurable *in vivo* using flortaucipir PET, T1-weighted MRI, and MRI with diffusion tensor imaging (DTI). However, little is known about how these processes relate to each other. The aim of this study was to investigate multimodal associations between flortaucipir PET uptake, tissue volume loss on structural MRI and white matter tract disruption on DTI. Thirty-four patients with progressive supranuclear palsy and 29 normal controls underwent flortaucipir PET, MRI and DTI. Voxel-wise comparison was performed between patients and controls. Sparse canonical correlations analysis was applied on regional measurements of flortaucipir uptake, tissue volume, fractional anisotropy and mean diffusivity of the PSP population. Pearson's correlation coefficients were assessed across modalities on the regions identified by the sparse canonical correlation analyses. Sparse canonical correlation analyses identified associations between elevated flortaucipir uptake in the cerebellar dentate, red nucleus and subthalamic nucleus and decreased volume in the same regions, and decreased fractional anisotropy and increased mean diffusivity in tracts including the superior cerebellar peduncle, sagittal striatum and posterior corona radiata. Furthermore, decreased fractional anisotropy and increased mean diffusivity in the body of the corpus callosum and anterior and superior corona radiata were related to volume loss in the frontal lobe. Tau uptake measured by flortaucipir PET appears to be related to the neurodegenerative process of progressive supranuclear palsy, including reduced tissue volume and white matter tract degeneration.

1. Introduction

Progressive supranuclear palsy (PSP) is a neurodegenerative disease characterized by the deposition of four repeat (4R) tau inclusions in brainstem and basal ganglia, stereotypic patterns of atrophy involving midbrain, thalamus, basal ganglia, middle cingulate and premotor cortex [1,2], and white matter tract degeneration, involving the superior cerebellar peduncle, body of the corpus callosum, posterior thalamic radiations and association tracts, such as the superior longitudinal fasciculus [3–5]. Clinically, PSP patients most often present with PSP-Richardson's syndrome, characterized by postural instability, falls and vertical supranuclear gaze palsy, although they can also present with other PSP syndromes. The advent of positron emission tomography (PET) ligands that can bind to tau proteins and, hence, allow the *in vivo* imaging of tau pathology, has potential to be important in PSP, which is a primary tauopathy. The flortaucipir tau-PET ligand has received the most attention thus far, and studies have shown that flortaucipir uptake is elevated in PSP in key regions, such as the dentate nucleus of the cerebellum, midbrain, pallidum and thalamus [6–8]. It has also been demonstrated that flortaucipir uptake increases over time in PSP [9]. However, autoradiographic studies have cast some doubt on whether flortaucipir is actually binding to 4R tau proteins in PSP [10–12]. Furthermore, the majority of studies have failed to identify any relationship between flortaucipir uptake and clinical disease severity [6,7,13], suggesting it may not be a good biomarker of underlying disease in PSP.

Understanding whether and how PSP multimodal neuroimaging markers are related to each other is a crucial next step, particularly to help determine potential neurodegenerative disease pathways, necessary for the development of effective therapies. Furthermore, it is currently unknown whether flortaucipir uptake is related to degeneration of the PSP system of grey matter regions and white matter tracts.

* Corresponding author. Mayo Clinic 200 1st St SW, Rochester, MN, 55905, USA
E-mail address: Sintini.Irene@mayo.edu (I. Sintini).

https://doi.org/10.1016/j.parkreldis.2019.07.001
Received 27 March 2019; Received in revised form 4 June 2019; Accepted 1 July 2019

Demonstrating that PSP flortaucipir uptake is related to neurodegeneration may help strengthen the argument that it is binding to something related to the disease process.

Accordingly, the aim of this study was to investigate regional associations between flortaucipir uptake, tissue volume measured on structural MRI, and white matter tract integrity measured on diffusion tensor imaging (DTI), using multimodal sparse canonical correlation analysis (SCCA) in a cohort of 34 patients with PSP.

2. Methods

2.1. Participants

Thirty-four patients with probable PSP had been recruited into an NIH-funded study (Co-PI's Josephs/Whitwell) and underwent a neurological evaluation, flortaucipir PET, 3T volumetric MRI and DTI. The time interval between the scans was one day. All patients had been identified from the Department of Neurology, Mayo Clinic, Rochester, MN. Of the 34 patients, 27 met clinical criteria for PSP-Richardson's syndrome, three for PSP-parkinsonism, two for PSP corticobasal syndrome, and two for PSP progressive gait freezing [14]. The median age at time of imaging was 71 years (IQR: 65,74) and 56% of participants were female. Median age at disease onset was 67 years (63,70) and the median disease duration was 3.3 years (2.0,4.8). All patients underwent a neurological examination by a Movement Disorder or Behavioral Neurologist (KAJ, HB or FA), which included testing using the PSP Rating Scale (median (IQR): 42.0 (36.3,48.0)), Movement Disorder Society Sponsored Revision of the Unified Parkinson's Disease Rating Scale part III (41.0 (34.5,46.8)), PSP oculomotor impairment scale (3 (2,4)), Montreal Cognitive Assessment Battery (25.0 (22.3,27.0)), and Frontal Assessment Battery (14 (13,16)). Twenty-nine healthy individuals were also recruited and used as controls. They had median age of 73 years (59,75) and 58% were female. Median score on the Mini-Mental State Examination was 29 (29,30). The study was approved by the Mayo Clinic IRB and all patients consented to participate in the study.

2.2. Neuroimaging

Flortaucipir PET scans were acquired using a PET/CT scanner (GE Healthcare, Milwaukee, Wisconsin) operating in 3D mode. An intravenous bolus injection of approximately 370 MBq (range 333–407 MBq) of flortaucipir was administered, followed by a 20 min PET acquisition performed 80 min after injection. Flortaucipir scans consisted of four 5-min dynamic frames following a low dose CT transmission scan. Standard corrections were applied. Emission data was reconstructed into a 256 × 256 matrix with a 30-cm field of view (FOV) (in-plane pixel size = 1.0 mm, slice thickness = 1.96 mm). The 3T head MRI protocol included: a magnetization prepared rapid gradient echo (MPRAGE) sequence TR/TE/TI, 2300/3/900 ms; flip angle 8°, 26-cm FOV; 256 × 256 in-plane matrix with a phase FOV of 0.94, and slice thickness of 1.2 mm; a DTI acquisition consisting of a single shot echo-planar (EPI) pulse sequence in the axial plane, with approximate TE 64 ms; TR = 10s; in-plane matrix 128/128; FOV 35 cm; phase FOV = 0.66; 41 diffusion encoding directions (b = 1000) and five non-diffusion weighted (b = 0) T2 images; slice thickness 2.7 mm (2.7 mm isotropic resolution); parallel imaging with a SENSE factor of two was used. MRI acquisitions were performed on a GE scanner (GE Healthcare, Milwaukee, Wisconsin).

Each flortaucipir PET image was rigidly registered to its corresponding MPRAGE using SPM12 (Wellcome Trust Centre for Neuroimaging, London, UK). Using ANTs, the Mayo Clinic Adult Lifespan Template (MCALT) (https://www.nitrc.org/projects/mcalt/) atlases were propagated to the native MPRAGE space and used to calculate regional PET values in grey and white matter regions-of-interest (ROIs). Tissue probabilities were determined for each MPRAGE using Unified Segmentation in SPM12, with MCALT tissue priors and settings. We selected ROIs to cover the entire cortex and subcortical grey matter structures, and also specific nuclei that are typically affected in PSP [15]. The cortical ROIs included frontal and sensorimotor regions that have been shown to be affected on neuroimaging in PSP (supplemental motor area; precentral; postcentral; paracentral; mid-cingulate; superior, middle and inferior frontal; medial frontal; orbitofrontal) and macro-ROIs covering regions that are less affected in PSP (medial and lateral temporal; parietal; occipital). Subcortical grey matter structures assessed included the pallidum, putamen, caudate, and thalamus. All cortical and subcortical ROIs were defined using MCALT. The midbrain, superior cerebellar peduncle, and cerebellum dentate were manually drawn on the MCALT atlas, as previously described [9]. The subthalamic nucleus, red nucleus and substantia nigra ROIs were defined using the Deep Brain Stimulation Intrinsic atlas [16]. Left and right ROIs were combined. This process resulted in 26 bilateral ROIs. Median flortaucipir PET value in each ROI was divided by median uptake in cerebellar crus grey matter to create standard uptake value ratios (SUVR). PET images were not partial volume corrected in order to keep MRI and PET measurements relatively independent from each other for the multimodal analyses. Tissue volume (grey and white matter) was calculated in same set of ROIs and normalized with respect to the total intracranial volume. The DTI images (fractional anisotropy (FA) and mean diffusivity (MD)) were processed as described in a previous study [17] and the median DTI scalar values (FA, MD) were measured within all of the specific white matter tract ROIs (27 in total, excluding lobar white matter regions) in the Johns Hopkins University atlas. The MRI, PET and DTI ROIs included in the multimodal analyses are shown in Supplemental Figure 1.

Structural MRI, DTI and PET images of each subject were subsequently spatially normalized to the MCALT template and blurred with an 8 mm (MRI, DTI) or 6 mm (PET) full width at half maximum kernel for voxel-wise analyses.

2.3. Statistical analysis

SPM12 was used to perform voxel-wise multiple regression analyses that assessed differences in flortaucipir PET uptake, MRI grey and white matter, DTI-FA and DTI-MD between PSP and controls. Age was included as a covariate and results were assessed both uncorrected and corrected for multiple comparisons using the family wise error (FWE) correction. SCCA was applied to investigate multivariate relationships between flortaucipir SUVR, tissue volume, DTI-FA and DTI-MD regional measurements within the PSP group. SCCA is an unsupervised multivariate method that seeks linear combinations of the variables in two datasets (i.e. ROIs from two different imaging modalities) by projecting them onto dimensions where they are maximally correlated to each other, using canonical weights [18]. SCCA is appropriate for high-dimensional datasets, i.e. large number of ROIs, because it identifies only the key ROIs that contribute to the associations between two imaging modalities. The effect of age was removed from the data by calculating the residuals, which are the difference between the measured values and the values predicted by a regression model. The SCCA dimension associated to the highest correlation coefficient was selected. Partial Pearson's correlations, with age as correcting factor, were performed between the regional quantities associated to the highest canonical weights in each SCCA, in the PSP patients as well as in the normal controls. Fisher's Z transformation was applied to assess statistically significant differences between the correlations in PSP and controls.

3. Results

3.1. Voxel-wise analyses

PSP showed patterns of reduced subcortical grey matter volume in caudate, putamen, thalamus, and midbrain, relative to controls; in the

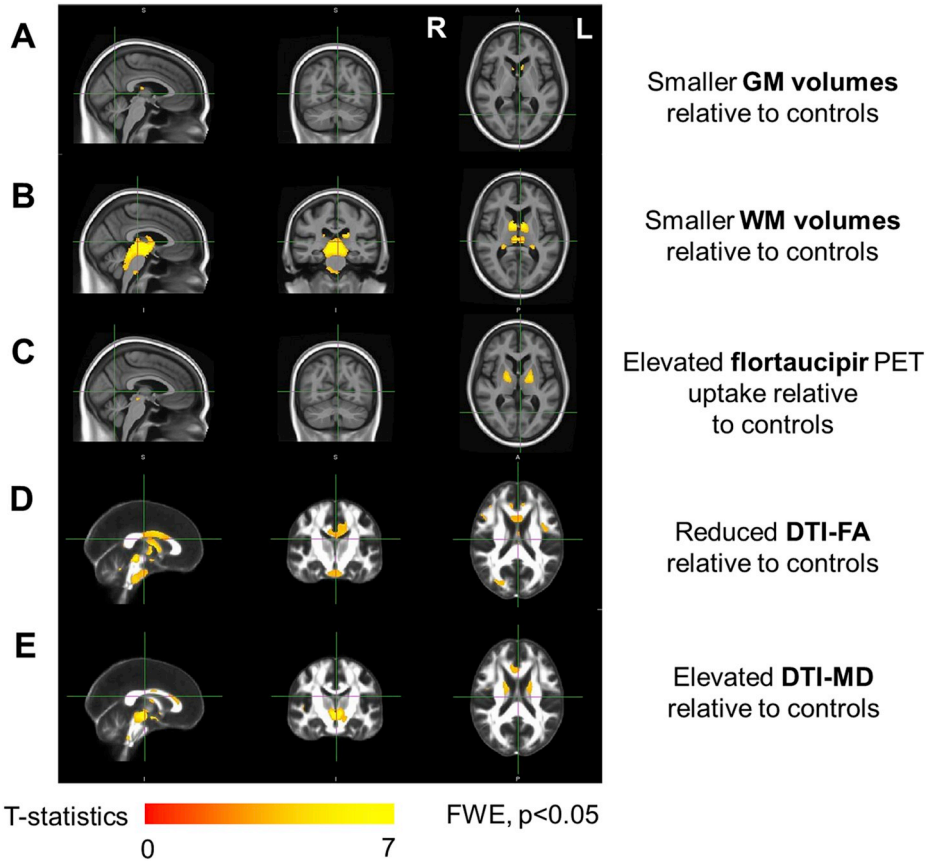

Fig. 1. Patterns of grey matter (GM) (A) and white matter (WM) (B) volume loss, elevated flortaucipir PET uptake (C), and tract degeneration (D, E) in the PSP cohort compared to controls. Results are shown after FWE correction at $p < 0.05$.

cortex, reduced volume was present in supplemental motor area, temporal pole and middle frontal gyrus, however these regions were not statistically significant after FWE correction (Fig. 1A, Supplemental Figure 2A). PSP showed reduced white matter volume relative to controls in midbrain, subthalamic nucleus, substantia nigra and superior cerebellar peduncle; white matter loss was present in frontal and supplemental motor areas but was not statistically significant after FWE correction (Fig. 1B, Supplemental Figure 2B). Patterns of elevated flortaucipir PET signal in PSP relative to controls were noted in cerebellar dentate, midbrain, red nucleus, subthalamic nucleus, thalamus, putamen, pallidum and caudate and most of these results were statistically significant after FWE correction (Fig. 1C, Supplemental Figure 2C). Analogous patterns were identified with partial volume correction (Supplemental Figure 2D). On DTI, PSP showed reduced FA relative to controls in several white matter tracts, including body of the corpus callosum, fornix, cerebellar peduncle, and elevated MD in midbrain, superior cerebellar peduncle, body of the corpus callosum and genu of corpus callosum (Fig. 1D–E, Supplemental Figure 3). No results were found in the opposite direction for white matter volume and DTI-MD; very few voxels in the opposite direction were present for flortaucipir PET uptake, grey matter volume and DTI-FA and they were not significant FWE correction at $p < 0.05$.

3.2. Multimodal regional analyses

SCCA identified strong associations between elevated flortaucipir SUVR, reduced tissue volume and white matter tract degeneration (Table 1, Supplemental Figure 4). Increased flortaucipir SUVR in red nucleus, subthalamic nucleus and cerebellar dentate and decreased volume in red nucleus, subthalamic nucleus and midbrain were related (Table 1), with the highest canonical weights assigned to the red nucleus for flortaucipir SUVR and the subthalamic nucleus for tissue volume ($R = -0.65$) (Fig. 2A, Table 2).

Increased flortaucipir SUVR was also related to decreased DTI-FA (Table 1), with the key regions being the cerebellar dentate for flortaucipir SUVR and the sagittal striatum for DTI-FA ($R = -0.53$) (Fig. 2B, Tables 1 and 2). Similarly, increased flortaucipir SUVR was related to increased DTI-MD (Table 1). The red nucleus was the region with the highest canonical weight for flortaucipir and the superior cerebellar peduncle had the highest canonical weight for DTI-MD ($R = 0.67$) (Fig. 2C, Table 2).

Decreased tissue volume in frontal regions was related to disruption of various tracts, including superior and anterior corona radiata and body of the corpus callosum (Table 1). Tissue volume in the inferior frontal ROI had an age-corrected Pearsons's correlation coefficient of $R = 0.60$ with the anterior corona radiata FA and of $R = -0.71$ with the superior corona radiata MD (Fig. 2D–E, Table 2).

The multimodal correlations coefficients on the top regions identified by SCCA were statistically different between PSP patients and controls, when tested with Fisher's Z transformation, for all the SCCA pairs except tissue volume with flortaucipir ($p = 0.07$).

4. Discussion

This study investigated regional associations between flortaucipir PET uptake, tissue volume loss from MRI and white matter tract degeneration from DTI in a large PSP population. Both flortaucipir uptake in the cerebellar dentate and midbrain regions and frontal volume loss showed distal correlations to degeneration in various white matter tracts, including the superior cerebellar peduncle, sagittal striatum, and superior and anterior corona radiata. Flortaucipir uptake in the cerebellar dentate and midbrain regions was also locally related to volume loss.

Table 1
Regions identified in the most highly correlated dimension of the sparse canonical correlation analysis for each modality-pair. The *R* coefficient is the Pearson's correlation coefficient between the two modalities, when projected onto the canonical dimensions, using the canonical weights. TV: tissue volume; FA: fractional anisotropy; MD: mean diffusivity. Regions associated to the highest canonical weight are in bold.

Modality 1	Modality 2	Modality 1 regions	Modality 1 wt	Modality 2 regions	Modality 2 wt	*R*
Flortaucipir	TV	**Red nucleus**	**0.93**	**Subthalamic nucleus**	**−0.92**	0.62
		Subthalamic nucleus	0.28	Red nucleus	−0.29	
		Cerebellar dentate	0.22	Midbrain	−0.25	
Flortaucipir	FA	**Cerebellar dentate**	**0.78**	**Sagittal striatum**	**−0.88**	0.61
		Red nucleus	0.62	Posterior corona radiata	−0.41	
		Substantia nigra	0.14	Superior longitudinal fasciculus	−0.24	
Flortaucipir	MD	**Red nucleus**	**0.87**	**Superior cerebellar peduncle**	**0.93**	0.64
		Cerebellar dentate	0.49	Fornix - stria terminalis	0.32	
				Posterior limb of internal capsule	0.17	
				Medial lemniscus	0.11	
TV	FA	**Inferior frontal**	**−0.89**	**Anterior corona radiata**	**−0.88**	0.74
		Superior frontal	−0.34	Fornix	−0.35	
		Orbitofrontal	−0.30	Body of the corpus callosum	−0.33	
TV	MD	**Inferior frontal**	**−0.96**	**Superior corona radiata**	**0.83**	0.79
		Superior frontal	−0.19	Body of the corpus callosum	0.52	
		Mid frontal	−0.14	Cingulate gyrus	0.21	
		Orbitofrontal	−0.11			
		Precentral	−0.11			

Voxel-wise analyses identified a distinct pattern of elevated flortaucipir uptake in PSP relative to controls, in the thalamus, basal ganglia, subthalamic nucleus, cerebellar dentate and midbrain regions, which typically show tau at autopsy [19], consistent with the literature [6,7]. Since some subcortical structures are subject to age-related accumulation of flortaucipir, we included age as a covariate in all our analyses to ensure that the increased flortaucipir signal was indeed a specific feature of the disease and not due to aging. Mild cortical flortaucipir uptake was observed in the frontal lobes but did not survive correction for multiple comparisons. Our cohort also showed the expected patterns of tissue volume loss in the midbrain, superior cerebellar peduncle, thalamus, subthalamic nuclei and basal ganglia. We found local correlations between reduced tissue volume and elevated flortaucipir signal in the red nucleus and subthalamic nucleus. Elevated flortaucipir signal in the cerebellar dentate was also found to correlate with volume loss in these midbrain and subthalamic structures. This suggests that flortaucipir uptake is related to the PSP neurodegenerative process, and we could hypothesize that tau deposition may be causing neurodegeneration in these regions. Indeed, pathological studies have shown that tau-positive neurofibrillary tangles and coiled bodies are associated with neuronal loss and midbrain atrophy in PSP [20,21]. The fact that we did not observe any correlations between flortaucipir uptake and reduced tissue volume in the basal ganglia or thalamus may support the view that flortaucipir in these regions reflects, or partially reflects, age-related off-target binding [22].

White matter tract disruption is a hallmark of neuropathological change in PSP. As expected, we found a decline in fractional anisotropy and an increase mean diffusivity in PSP patients relative to controls [4,5,23]. PSP is characterized by disruption of the dentatorubrothalamic tract, which connects the cerebellar dentate to the thalamus, through the red nucleus and superior cerebellar peduncle, and its projections from the ventrolateral thalamus terminate in the premotor and motor cortices [3]. Recent studies proved that the pathological involvement of the dentatorubrothalamic tract is indeed a diagnostic feature of PSP and can help differentiate this syndrome from Parkinson's disease [24,25]. Our analyses showed that the degeneration of the dentatorubrothalamic tract was related to both the accumulation of flortaucipir uptake and the reduction of tissue volume in the PSP-related areas of the brain. This strengthens the possibility that degeneration of tracts like the superior cerebellar peduncle, superior longitudinal fasciculus, posterior corona radiata and sagittal striatum could be related to the presence of tau pathology in the cerebellar dentate, red nucleus and substantia nigra [8]. The superior cerebellar peduncle connects the cerebellum to the midbrain, while the superior longitudinal fasciculus projects into the posterior frontal lobe. These two tracts are located in areas of the brain very relevant to the process of neurodegeneration in PSP patients and their relation to flortaucipir uptake could suggest that flortaucipir uptake is indeed an important biomarker of the disease. Others have speculated that the superior cerebellar peduncle is particularly susceptible to tau pathology [26] and our results point in the same direction. Pathologically, the degree of myelin loss has indeed been shown to be associated to tau burden in the superior cerebellar peduncle [27]. The sagittal striatum conveys fibers from the cortex to subcortical destinations in the thalamus and brainstem structures, while the fibers of the superior corona radiata radiate out from the cortex and come together in the brainstem; our results suggest that their degeneration could be influenced by the presence of subcortical tau, as measured by flortaucipir PET. Degeneration of the internal capsule has been previously noted as a characteristic feature of PSP [23] and we found a correlation between flortaucipir uptake in the red nucleus and cerebellar dentate and increased mean diffusivity in this tract. We could therefore speculate that tau pathology is related to the whole degeneration system, i.e. volume loss and white matter tract disruption, which characterizes PSP. Additionally, from the close spatial relationships between white matter structural damage (superior cerebellar peduncle) and flortaucipir uptake (cerebellar dentate), one could even hypothesize that the tau results in disruption of the white matter tracts. While we found that infratentorial flortaucipir uptake was also related to degeneration of more distant white matter tracts in the frontal lobe, we did not find any relationship between flortaucipir uptake and reduced tissue volume in the frontal lobe. However, we did detect associations between reduced tissue volume in the frontal lobe and degeneration of several white matter tracts that have connections in the frontal lobe, like the anterior and superior corona radiata and the body of the corpus callosum. This may support the hypothesis that frontal atrophy in PSP occurs as a result of degeneration of the associated white matter tracts, rather than as a direct result of tau deposition, while tau deposition possibly starts in subcortical structures and drives the white matter tract degeneration.

A potential limitation of the present study is the clinical heterogeneity of our cohort, given that different clinical variants may show different regional multimodal relationships. We did not observe any striking differences in the multimodal imaging correlations across variants, although a larger patient cohort is needed to draw any conclusion, since the large majority of our patients were diagnosed with PSP-Richardson's syndrome. The inclusion of different syndromic

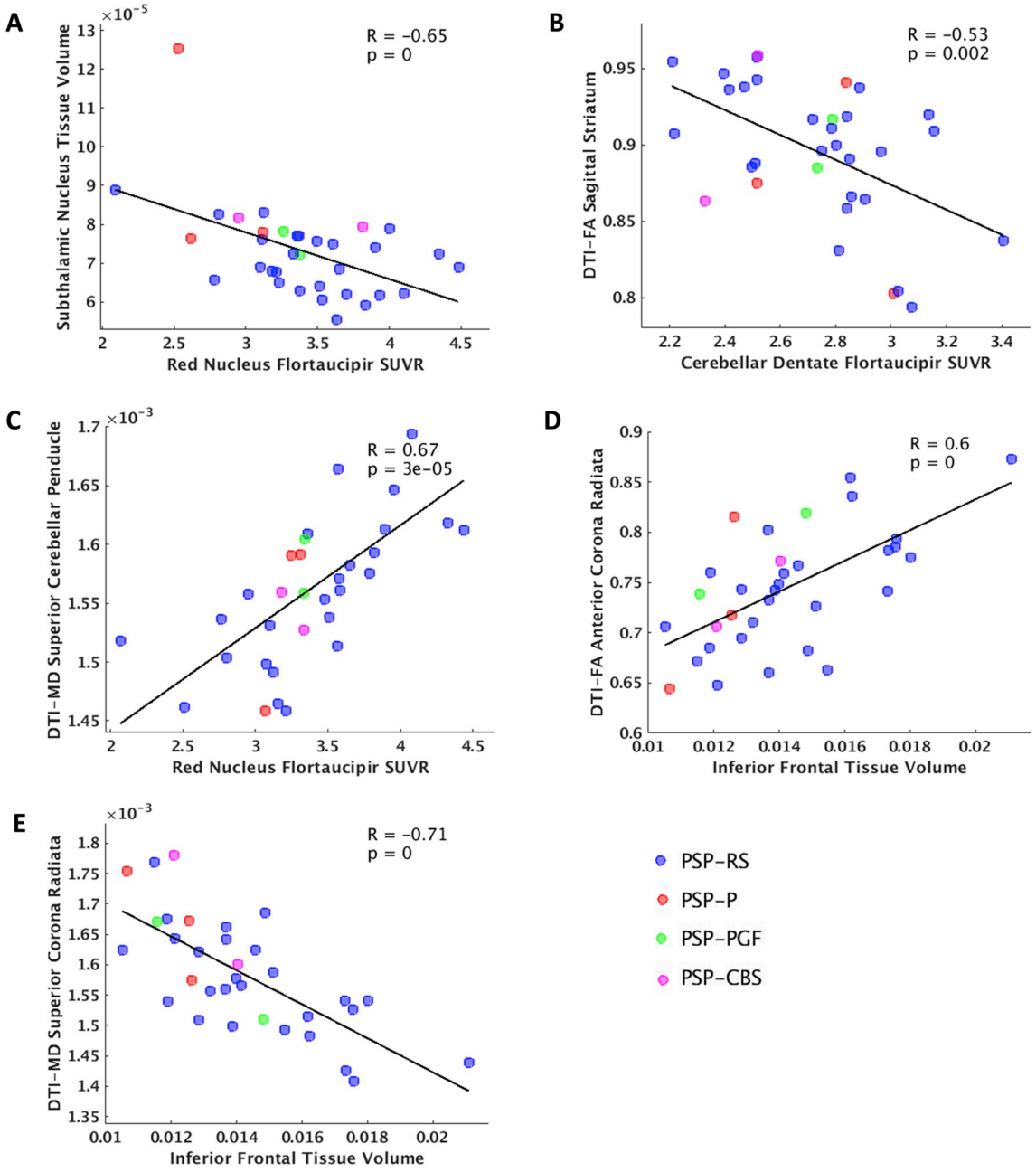

Fig. 2. Scatter plots showing the correlation between the regions with the highest canonical weights for each modality-pair. Each PSP variant is displayed in a different color: PSP-Richardson's syndrome (PSP-RS), PSP-parkinsonism (PSP–P), PSP-progressive gait freezing (PSP-PGF), and PSP-corticobasal syndrome (PSP-CBS). (For interpretation of the references to color in this figure legend, the reader is referred to the Web version of this article.)

Table 2
Age-corrected Pearson's correlation coefficients between variables with highest canonical weights for PSP patients and controls. TV: tissue volume; FA: fractional anisotropy; MD: mean diffusivity.

Modality 1	Modality 2	*R*in PSP	*R*in controls	Fisher's p value
Red nucleus flortaucipir	Subthalamic nucleus TV	−0.65	−0.29	0.07
Cerebellar dentate flortaucipir	Sagittal striatum FA	−0.53	0.36	0.03
Red nucleus flortaucipir	Superior cerebellar peduncle MD	0.67	0.26	0.05
Inferior frontal TV	Anterior corona radiata FA	0.60	0.09	0.01
Inferior frontal TV	Superior corona radiata MD	−0.71	−0.35	0.05

variants likely explains why our cohort is a few years older than previously reported PSP-Richardson's syndrome cohorts (typically ~ 68 years) [3]. Regarding our methods, SCCA has been effectively implemented to uncover sensible multivariate associations among neuroimaging modalities in neurodegenerative diseases [28,29]. However, it must be stressed that this statistical method can identify only linear relationships and one should be careful when drawing conclusions on causality. Other existing statistical techniques might find

different relationships in the same data. Finally, we must note that, although SCCA uncovered many PSP-specific multimodal associations, it did also identify some regions that are not typically specific to this disease, such as the fornix. To corroborate the findings of the current study and uncover more PSP-specific relationships, a larger cohort of patients would be beneficial.

There is also a great deal of uncertainty concerning whether flortaucipir is binding to underlying 4R tau in PSP. This ligand was originally developed for Alzheimer's disease, characterized by paired helical filaments of 3R + 4R tau, while tau pathology in PSP is characterized by straight filaments of 4R tau. However, a number of studies have found good correlations between flortaucipir uptake and 4R tau burden at autopsy [7,30,31]. Although we must note that the most significant difference between PSP patients and controls was in the association concerning tissue volume loss and decline in fractional anisotropy, our current findings, along with those of a previous study that found correlations between flortaucipir uptake and functional connectivity in PSP [32], strengthen the idea that tau-PET imaging with the tracer flortaucipir could provide a disease biomarker useful for clinical treatment trials for PSP.

Financial disclosures

Dr.'s Whitwell, Josephs, Ali, Botha and Schwarz receive funding from the NIH. Matthew Senjem owns stock in Align Technology, Inc, Gilead Sciences, Inc., Globus Medical Inc., Inovio Biomedical Corp., Johnson & Johnson, LHC Group, Inc., Medtronic, Inc., Mesa Laboratories, Natus Medical Incorporated, Oncothyreon, Inc., Parexel International Corporation, Varex Imaging Corporation. Dr. Lowe serves is a consultant for Bayer Schering Pharma, Philips Molecular Imaging, Piramal Imaging and GE Healthcare and receives research support from GE Healthcare, Siemens Molecular Imaging, AVID Radiopharmaceuticals, the NIH (NIA, NCI), and the MN Partnership for Biotechnology and Medical Genomics. Dr. Jack serves on a scientific advisory board for Eli Lilly & Company and on an independent data safety monitoring board for Roche but he receives no personal compensation from any commercial entity. He receives research support from the NIH, and the Alexander Family Alzheimer's Disease Research Professorship of the Mayo Clinic.

Funding source

NIH R01-NS89757, R01-DC12519 and R21-NS94684.

Acknowledgments

The study was funded by the National Institutes of Health, grants R01-NS89757, R01-DC12519 and R21-NS94684. We would like to greatly thank Avid Radiopharmaceuticals, for their support in supplying the AV-1451 precursor, chemistry production advice and oversight, and FDA regulatory cross-filing permission and documentation needed for this work.

Appendix A. Supplementary data

Supplementary data related to this article can be found at https://doi.org/10.1016/j.parkreldis.2019.07.001.

References

[1] K.A. Josephs, et al., Modeling trajectories of regional volume loss in progressive supranuclear palsy, Mov. Disord. 28 (8) (2013) 1117–1124.
[2] S. Price, et al., Voxel-based morphometry detects patterns of atrophy that help differentiate progressive supranuclear palsy and Parkinson's disease, Neuroimage 23 (2) (2004) 663–669.
[3] J.L. Whitwell, et al., Disrupted thalamocortical connectivity in PSP: a resting state fMRI, DTI, and VBM study, Park. Relat. Disord. 17 (8) (2011) 599–605.
[4] J.L. Whitwell, et al., Clinical correlates of white matter tract degeneration in progressive supranuclear palsy, Arch. Neurol. 68 (6) (2011) 753–760.
[5] E. Canu, et al., Diffusion tensor magnetic resonance imaging tractography in progressive supranuclear palsy, Mov. Disord. 26 (9) (2011) 1752–1755.
[6] L. Passamonti, et al., F-18-AV-1451 positron emission tomography in Alzheimer's disease and progressive supranuclear palsy, Brain 140 (2017) 781–791.
[7] D.R. Schonhaut, et al., F-18-flortaucipir tau positron emission tomography distinguishes established progressive supranuclear palsy from controls and Parkinson disease: a multicenter study, Ann. Neurol. 82 (4) (2017) 622–634.
[8] J.L. Whitwell, et al., [18 F]AV-1451 tau positron emission tomography in progressive supranuclear palsy, Mov. Disord. 32 (1) (2017) 124–133.
[9] J.L. Whitwell, et al., MRI outperforms [18F]AV-1451 PET as a longitudinal biomarker in progressive supranuclear palsy, Mov. Disord. 34 (2019) 105–113.
[10] V.J. Lowe, et al., An autoradiographic evaluation of AV-1451 Tau PET in dementia, Acta Neuropathol. Commun. 4 (1) (2016) 58.
[11] M. Marquie, et al., Validating novel tau positron emission tomography tracer [F-18]-AV-1451 (T807) on postmortem brain tissue, Ann. Neurol. 78 (5) (2015) 787–800.
[12] K. Sander, et al., Characterization of tau positron emission tomography tracer [18F]AV-1451 binding to postmortem tissue in Alzheimer's disease, primary tauopathies, and other dementias, Alzheimer's Dementia 12 (11) (2016) 1116–1124.
[13] J.L. Whitwell, et al., Pittsburgh Compound B and AV-1451 positron emission tomography assessment of molecular pathologies of Alzheimer's disease in progressive supranuclear palsy, Park. Relat. Disord. 48 (2018) 3–9.
[14] G.U. Hoglinger, et al., Clinical diagnosis of progressive supranuclear palsy: the movement disorder society criteria, Mov. Disord. 32 (6) (2017) 853–864.
[15] J.L. Whitwell, et al., Radiological biomarkers for diagnosis in PSP: where are we and where do we need to Be? Mov. Disord. 32 (7) (2017) 955–971.
[16] S. Ewert, et al., Toward defining deep brain stimulation targets in MNI space: a subcortical atlas based on multimodal MRI, histology and structural connectivity, Neuroimage 170 (2018) 271–282.
[17] C.G. Schwarz, et al., Improved DTI registration allows voxel-based analysis that outperforms Tract-Based Spatial Statistics, Neuroimage 94 (2014) 65–78.
[18] D.M. Witten, R. Tibshirani, T. Hastie, A penalized matrix decomposition, with applications to sparse principal components and canonical correlation analysis, Biostatistics 10 (3) (2009) 515–534.
[19] D. Dickson, R.O. Weller, Neurodegeneration: the Molecular Pathology of Dementia and Movement Disorders, John Wiley & Sons, 2011.
[20] C.H. Jin, et al., Relationship between neuronal loss and tangle formation in neurons and oligodendroglia in progressive supranuclear palsy, Neuropathology 26 (1) (2006) 50–56.
[21] I. Aiba, et al., Relationship between brainstem MRI and pathological findings in progressive supranuclear palsy - study in autopsy cases, J. Neurol. Sci. 152 (2) (1997) 210–217.
[22] J.Y. Choi, et al., Off-target F-18-AV-1451 binding in the basal ganglia correlates with age-related iron accumulation, J. Nucl. Med. 59 (1) (2018) 117–120.
[23] A. Padovani, et al., Diffusion tensor imaging and voxel based morphometry study in early progressive supranuclear palsy, J. Neurol. Neurosurg. Psychiatry 77 (4) (2006) 457–463.
[24] S. Nigro, et al., Track density imaging in progressive supranuclear palsy: a pilot study, Hum. Brain Mapp. 40 (6) (2019) 1729–1737.
[25] M. Seki, et al., Diagnostic potential of dentatorubrothalamic tract analysis in progressive supranuclear palsy, Park. Relat. Disord. 49 (2018) 81–87.
[26] F. Agosta, et al., Tracking brain damage in progressive supranuclear palsy: a longitudinal MRI study, J. Neurol. Neurosurg. Psychiatry 89 (7) (2018) 696–701.
[27] K. Ishizawa, et al., A qualitative and quantitative study of grumose degeneration in progressive supranuclear palsy, JNEN (J. Neuropathol. Exp. Neurol.) 59 (6) (2000) 513–524.
[28] B.B. Avants, et al., Dementia induces correlated reductions in white matter integrity and cortical thickness: a multivariate neuroimaging study with sparse canonical correlation analysis, Neuroimage 50 (3) (2010) 1004–1016.
[29] I. Sintini, et al., Longitudinal tau-PET uptake and atrophy in atypical Alzheimer's disease, Neuroimage: Clinical 23 (2019) 101823.
[30] K.A. Josephs, et al., [18F]AV-1451 tau-PET uptake does correlate with quantitatively measured 4R-tau burden in autopsy-confirmed corticobasal degeneration, Acta Neuropathol. 132 (6) (2016) 931–933.
[31] C.T. McMillan, et al., Multimodal evaluation demonstrates in vivo F-18-AV-1451 uptake in autopsy-confirmed corticobasal degeneration, Acta Neuropathol. 132 (6) (2016) 935–937.
[32] T.E. Cope, et al., Tau burden and the functional connectome in Alzheimer's disease and progressive supranuclear palsy, Brain 141 (2018) 550–567.